

Cosmological phase transitions from the functional measure

Bruno Berganholi¹, Gláuber C. Dorsch^{1,*}, Iberê Kuntz², Beatriz M. D. Sena¹, and Giovanna F. do Valle¹

¹*Departamento de Física, Universidade Federal de Minas Gerais (UFMG), Belo Horizonte, MG, Brazil*

²*Departamento de Física, Universidade Federal do Paraná (UFPR), Curitiba, PR, Brazil*

We investigate how competitive gravitational wave detectors can be to current and near-future colliders in probing a model where the new physics is completely encapsulated in a modified scalar sector. For this, we study a model where an additional logarithmic term arises in the scalar potential due to a non-trivial path integral measure, which is constructed using effective field theory. This new term alters the dynamics of cosmological phase transitions and could lead to potentially detectable gravitational waves from the early Universe. Our results confirm the expectation that the intensity of such spectrum is highly correlated to the scalar field's self-coupling, and that gravitational wave experiments could therefore be used to probe these couplings with an accuracy competitive with the projected sensitivity of near-future colliders.

I. INTRODUCTION

Since the dawn of high energy physics, particle accelerators have continuously reinforced their status as *the* paradigmatic tools for testing our models of fundamental particle interactions. However, the initial success of the LHC program in detecting the Higgs boson has so far been followed by a disturbing silence regarding concrete signs of new physics, despite prior expectations to the contrary. At the same time, the last decade has been marked by the inaugural direct detection of gravitational wave (GW) signals, even coming from experiments employing considerably different detection techniques, such as interferometers [1–4] and pulsar timing arrays [5, 6]. These experiments open a new window for exploring our cosmos, and could even be employed as new probes for testing particle physics models. Most importantly, they could bring new information on the high energy frontier, competitive with or even complementary to those coming from colliders [7]. This is especially the case for models where the new physics affects mostly (or exclusively) the scalar sector, since probing the details of the Higgs potential involves measuring its self-couplings, which is a formidable task for current colliders [8], and challenging even at accelerators projected for the near-future [9–11].

An interesting example of these types of models can be found in the recent literature. It has been noted that the definition of the functional measure in the partition function of quantum field theories largely depends on the geometry of configuration space, and adopting the Riemannian measure amounts to effectively adding a logarithmic correction to the scalar potential [12, 13]. This new term leads to a correction of the Higgs quartic coupling as well as to $\mathcal{O}(\phi^6/\Lambda^2)$ operators (with Λ some cutoff scale). Recent works have shown that this effect has no impact on electroweak precision observables [13], so the most immediate direct probe at colliders would be via the modified Higgs trilinear couplings¹. At the

same time, such a modification of the scalar potential could have a drastic impact on the cosmic evolution of the Universe, even altering the nature of the electroweak phase transition, and leading to a potentially detectable GW spectrum in near-future interferometers.

The purpose of this work is to investigate the cosmological impact of a non-trivial Riemannian functional measure, and explore the possibility of probing these effects with GW detectors. We will see that future interferometers, such as LISA, DECIGO and BBO, could be sensitive to new logarithmic terms in the effective potential. This can be translated into bounds on the trilinear coupling, and we will show that future GW experiments could probe these at a competitive level if compared to the projected sensitivity of near-future experiments.

This is important because we are living in an era where a number of GW experiments are under the spotlight, and many others are receiving increasing attention and funding, so it is all the more important that we harness the capabilities of these machines to probe particle physics as well. In a recent work we have illustrated how direct particle detectors and GW interferometers could provide *complementary* information on models with dark sectors [7]. Here we show how *competitive* these GW experiments can be as compared to near-future colliders for probing the Higgs self-couplings if the new physics is exclusively in the scalar sector. However, it is important to emphasize at the outset that investing on both fronts (i.e. GW detectors and colliders) will remain essential for the progress of particle physics in the near future, especially at this moment when we still know little about the actual character of this BSM physics.

The paper is organized as follows. In section II we review the issue of defining an integration measure in field space and show that a redefinition of this quantity in the partition function amounts to adding a logarithmic correction to the effective scalar potential. Section III is dedicated to discussing the physicality conditions one

* glauber@fisica.ufmg.br

¹ Directly probing the quartic couplings or deviations from an ef-

fective ϕ^6 operator would be rather hopeless in near-future colliders, as argued above.

can impose on the model. In section IV we introduce the thermal corrections and discuss the dynamics of the phase transition and its relevant parameters, which leads to gravitational wave production and its potential detection at future interferometers such as LISA, DECIGO and BBO, discussed in section V. Our results are shown in section VI, and our conclusions are reserved for section VII.

II. FUNCTIONAL MEASURE IN QUANTUM FIELD THEORY

Path integrals have long become part of the arsenal of every field theorist, with applications ranging from condensed matter to high-energy physics. The functional approach shines, in particular, when applied to gauge theories as it preserves manifested Lorentz covariance and gauge invariance. Path integrals are also a centerpiece in Wilson's modern formulation of effective field theory, which could be taken as the proper definition of quantum field theory [14, 15].

In Wilson's approach, the theory is finite and defined at energies $\Lambda < \Lambda_{\text{phys}}$ below some physical scale Λ_{phys} ²:

$$Z_{\Lambda}[J] = \int_{\Omega(\Lambda)} d\mu[\varphi] e^{-(S[\varphi] + J_i \varphi^i)}, \quad (1)$$

where $S[\varphi]$ is the Euclidean classical action for some arbitrary field φ^i and J_i is the external current. Here $\Omega(\Lambda)$ is the integration domain that includes modes with energy below Λ . The physical scale Λ_{phys} , such as the interatomic scale in condensed matter or the Planck length in high-energy physics, acts as a true regulator at high energies. Unlike the ordinary approach to quantum field theory, Λ_{phys} prevents UV divergences from appearing, making the theory finite from the onset. Renormalization in this context is just a statement about the independence of observables under changes in Λ :

$$\Lambda \frac{dZ_{\Lambda}[J]}{d\Lambda} = 0. \quad (2)$$

Although Wilson's effective field theory resolves some conceptual issues regarding the definition of quantum field theory (it is finite after all), the integration measure $d\mu[\varphi]$ remains an obscure object [16–24]. The majority of the literature just take this measure to be trivial:

$$\mathcal{D}\varphi^i = \prod_i d\varphi^i. \quad (3)$$

² We are adopting DeWitt's index convention by merging continuous (spacetime coordinates) and discrete indices (denoted by capital letters) into small indices $i = (x, I)$. For example, if $\varphi^i = A_{\mu}^a(x)$ is a vector field, $i = (x, \{\mu, a\})$. Repeated small indices then implicitly contain sums over discrete indices and integrations over spacetime.

The choice of the integration measure, however, depends on geometrical and topological aspects of the configuration space. Even if one takes the natural choice, namely the measure induced by the underlying topology, it is unlikely that Eq. (3) will suffice in general. For one, fields can be singular (either diverge or not be defined) at some regions, which already shows that the configuration space is not simply connected. The presence of constraints, such as in gauge theories, would also make the configuration-space topology non-trivial, preventing the use of the trivial measure (3). These non-trivial characteristics of the configuration space are inherited from the phase space structure implied by the canonical quantization (see the Appendix of [13]).

From the theory of integration on manifolds, albeit we are working in the quite unusual setting of an infinite-dimensional manifold [25], the correct measure ought to be

$$d\mu[\varphi] = \mathcal{D}\varphi^i \sqrt{\text{Det } G_{ij}}. \quad (4)$$

Here $\text{Det } G_{ij}$ denotes the functional determinant, which includes the determinant of finite-dimensional operators (hereby denoted by \det), of the configuration-space metric G_{ij} . One should recall from differential geometry that the metric g is an additional structure independent of the underlying topological manifold \mathcal{M} . There are many possible metrics for the same \mathcal{M} , which results in different Riemannian manifolds (\mathcal{M}, g) for every choice of g . Incidentally, one faces the problem of choosing G_{ij} .

Typically, the configuration-space metric is identified from the action's kinetic term, as in non-linear sigma models [26–29]. In this approach, the measure can be used to cancel out ultralocal divergences [28, 29]. The function G_{IJ} are then defined from the kinetic term coefficients, namely:

$$\begin{aligned} & \int d^4x G_{IJ}(\varphi) \partial_{\mu} \varphi^I \partial^{\mu} \varphi^J \\ &= \int d^4x \int d^4x' G_{IJ}(\varphi) \delta^{(4)}(x - x') \frac{\partial \varphi^I(x)}{\partial x^{\mu}} \frac{\partial \varphi^J(x')}{\partial x'^{\mu}}, \end{aligned} \quad (5)$$

hence³

$$G_{ij} = G_{IJ}(\varphi) \delta^{(4)}(x - x'). \quad (6)$$

This proportionality with Dirac's delta is referred to as ultralocality and follows from the assumption of a local Lagrangian. This definition via the kinetic term can be justified when the phase-space measure

$$d\mu[\varphi, \Pi] = \mathcal{M}(\varphi, \Pi) \mathcal{D}\varphi^i \mathcal{D}\Pi_i \quad (7)$$

³ The configuration space \mathcal{C} is the set of all fields $\varphi^I(x)$. The set $\mathcal{N}_x \subset \mathcal{C}$ defined by all configurations at a fixed point x^{μ} is a finite-dimensional manifold. The function G_{IJ} is the metric over \mathcal{N} .

is trivial, i.e. $\mathcal{M}(\varphi, \Pi) \equiv 1$. In this case, the determinant factor in Eq. (4) follows upon integration over the canonical momentum Π_i . This argument also relies on the Gaussian integration, thus it cannot be applied to higher-derivative theories where higher powers of Π_i are present in the Hamiltonian.

Even when the measure is admittedly non-trivial, the standard practice appeals to dimensional regularization to trivialize it. The usual rationale goes by noting that

$$\text{Det } G_{ij} = \exp \left(\delta^{(n)}(0) \int d^n x \log \det G_{IJ} \right), \quad (8)$$

for any ultralocal metric of the form (6), and that scaleless integrals vanish in dimensional regularization, hence $\delta^{(n)}(0) = 0$ and $\text{Det } G_{ij} = 1$. This is an improper use of dimensional regularization because the argument of the exponential in Eq. (8) is the product of formally divergent quantities [25]. The integral in Eq. (8) can be divergent too, thus it must be carefully handled, together with the Dirac delta, before simply setting the exponential to unity. That is precisely the sort of undefined products one encounters when anomalies are present, in which case a naive use of dimensional regularization would erroneously hide the violation of classical symmetries [30–32]. We shall give another example of this later on.

We should stress that there is no universal choice for G_{ij} , which must be regarded as part of the theory's definition. Different metrics on the configuration space correspond to distinct quantization schemes. The complete specification of the theory is therefore given by the pair $(S[\varphi], G_{ij})$. Choosing different metrics for the same classical action leads to distinct quantum theories derived from the same classical framework.

The aforementioned approach, whereby one defines G_{ij} from the kinetic terms [26–29], is natural as the metric is induced by the most fundamental physical object, thus requiring only $S[\varphi]$ to fully specify the quantum theory. However, as we argued, this definition faces a number of limitations for not being applicable to higher-derivative theories or non-trivial phase spaces. Ref. [13] introduced a novel approach where the configuration-space metric G_{ij} is constructed using effective field theory, writing it as an infinite tower of invariant operators. From this perspective, the definition of G_{ij} is decoupled from the classical action $S[\varphi]$, but the same symmetry principles of effective field theory are adopted to define them both independently. This definition provides a reliable description at energies below the physical cutoff Λ_{phys} , irrespective of the exact functional measure required in a UV-complete theory. In this framework, the free parameters in G_{ij} influence the theory's phenomenology and can be determined through experimental observations [12, 13, 33, 34] rather than solely by their relationship to the kinetic term.

In this effective field theory approach, it is still reasonable to assume ultralocality as in Eq. (6) in order to prevent non-local behaviour. At some scale Λ , dimension

analysis gives

$$G_{ij}^\Lambda = G_{IJ}(\varphi/\Lambda) \delta_\Lambda^{(4)}(x - x'), \quad (9)$$

where $\delta_\Lambda^{(4)}(x - x')$ is the regularized Dirac delta. A smooth Wilsonian cutoff Λ can be implemented via the heat-kernel regularization⁴:

$$\delta_\Lambda^{(4)}(x) = \frac{\Lambda^4}{(2\pi)^2} e^{-\frac{x^2 \Lambda^2}{2}}, \quad (10)$$

so that

$$\delta_\Lambda^{(4)}(0) = \frac{\Lambda^4}{(2\pi)^2}. \quad (11)$$

We shall be interested in the scalar sector $\varphi^i = (\varphi(x), \varphi^\dagger(x))$ with $i = (\emptyset, x)$. Restricting to quadratic inverse powers of the cutoff, we find

$$G_{IJ} = \begin{pmatrix} c_1 + c_2 \frac{\varphi^\dagger \varphi}{\Lambda^2} & c_3 + c_4 \frac{\varphi^\dagger \varphi}{\Lambda^2} \\ c_5 + c_6 \frac{\varphi^\dagger \varphi}{\Lambda^2} & c_7 + c_8 \frac{\varphi^\dagger \varphi}{\Lambda^2} \end{pmatrix} + \mathcal{O}(\Lambda^{-3}), \quad (12)$$

where c_i are dimensionless free parameters. Note that there are no other terms invariant under $U(1)$ at this order. Eq. (8) can be readily computed:

$$\text{Det } G_{ij} = \exp \left[\frac{\Lambda^4}{(2\pi)^2} \int d^4 x \log \left(A + B \frac{\varphi^\dagger \varphi}{\Lambda^2} \right) \right], \quad (13)$$

where A, B are merely redefinitions of c_i . The integrand of (13) can be written as:

$$\Lambda^4 \log \left(A + B \frac{\varphi^\dagger \varphi}{\Lambda^2} \right) = \Lambda^4 \log A + \Lambda^2 \frac{B}{A} \varphi^\dagger \varphi \quad (14)$$

$$- \frac{1}{2} \frac{B^2}{A^2} (\varphi^\dagger \varphi)^2 + \mathcal{O}(\Lambda^{-2}). \quad (15)$$

We recall that in Wilson's effective field theory, the theory is finite by construction. However, even if one were to take $\Lambda \rightarrow \infty$ as in the ordinary view of renormalization, the positive powers of Λ in Eq. (15) would get cancelled out by the counter terms, the negative powers of Λ would go to zero, but the third term is cutoff-independent and remains finite after taking Λ to infinity. Therefore,

$$\text{Det } G_{ij} = \exp \left[-\frac{1}{4\pi^2} \frac{B^2}{A^2} \int d^4 x (\varphi^\dagger \varphi)^2 \right], \quad (16)$$

which shows that the functional measure cannot be neutralized by dimensional regularization. The correction

⁴ Other cutoff implementations, such as a hard cutoff or lattice regularization with lattice spacing Λ^{-1} , give the same functional dependence on Λ . The numerical factor in the denominator $(2\pi)^2$ is however regularization-dependent.

(16) provides a finite contribution to the renormalization of the quartic interaction, thus changing its renormalization group running. The same would also happen for higher-order coupling constants should one include higher-order operators in the metric (12). In such an expansion, one thus recovers all possible interactions that are already present in standard effective field theory (without a functional measure), but their corresponding coefficients are shifted. Clearly, this is only possible at the analytical regime of the logarithm in Eq. (13). The effects of $A = 0$, for example, cannot be reproduced by any finite order of the ordinary effective field theory expansion. They correspond to truly non-perturbative effects.

Plugging Eqs. (13) and (4) into (1), one sees that the effect of this modified integration measure in field space can be rephrased as a shift in the effective potential, such that⁵ [13]

$$V_{\text{eff}} = V_{\text{cl}} - \frac{\Lambda^4}{8\pi^2} \log \left(A + B \frac{\varphi^\dagger \varphi}{\Lambda^2} \right), \quad (17)$$

where V_{cl} is the classical scalar potential. In this work we are interested in the cosmological consequences of this additional contribution to the scalar potential. Since we have added a minimal modification to the trivial metric, cf. eq. (12), we will dub this the *minimal modified functional measure model* (or MMFMM).

III. ZERO TEMPERATURE EFFECTIVE POTENTIAL AND PHYSICALITY CONDITIONS

Let us assume a Higgs-like field governed by a potential (at the classical level) given by

$$V_{\text{cl}}(\varphi) = -\mu^2 \varphi^\dagger \varphi + \lambda (\varphi^\dagger \varphi)^2. \quad (18)$$

Quantum corrections to this potential include the typical Coleman-Weinberg terms at 1-loop level, and also the quantum correction due to the modified integration measure. Apart from an overall constant, the latter can be rewritten such that the 1-loop zero-temperature effective potential becomes

$$\begin{aligned} V^{(1)}(\phi, T=0) &= -\frac{\mu^2}{2} \phi^2 + \frac{\lambda}{4} \phi^4 \\ &+ \sum_i (-1)^{s_i} n_i \frac{m_i(\phi)^4}{64\pi^2} \left(\ln \frac{m_i^2(\phi)}{Q^2} - \frac{1}{2} \right) \\ &- \frac{\Lambda^4}{8\pi^2} \ln \left(1 - C \frac{\phi^2}{\Lambda^2} \right) \end{aligned} \quad (19)$$

where the sum in i runs over all vector bosonic ($s_i = 0$) and fermionic ($s_i = 1$) degrees of freedom running in the

loops, and we defined $\varphi \equiv \phi/\sqrt{2}$ and $C \equiv -B/2A$. For the mass of the W boson we take 80.36 GeV, while for the Z boson we use 91.19 GeV, and for the top quark 173.1 GeV. The contributions from the masses of other particles are negligible and were therefore disregarded.

The parameters μ and λ are fixed at the electroweak scale by imposing that the Higgs potential has a minimum at $v = 246$ GeV and that its mass is $m_h = 125$ GeV, i.e. $\partial V^{(1)}/\partial \phi|_{\phi=v} = 0$ and $\partial^2 V^{(1)}/\partial \phi^2|_{\phi=v} = m_h^2$ ⁶. Thus the full effective potential can be rewritten as

$$\begin{aligned} V^{(1)}(\phi, 0) &= \frac{m_h^2}{8v^2} (\phi^2 - v^2)^2 \\ &+ \sum_i \frac{n_i g_i^4}{64\pi^2} \left(\phi^4 \left(\ln \frac{\phi^2}{v^2} - \frac{3}{2} \right) + 2\phi^2 v^2 \right) \\ &- \frac{\Lambda^4}{8\pi^2} \ln \left(1 - C \frac{\phi^2}{\Lambda^2} \right) \\ &- \frac{C\Lambda^2}{4\pi^2} \frac{1 - 2Cv^2/\Lambda^2}{(1 - Cv^2/\Lambda^2)^2} \frac{\phi^2}{2} \\ &- \frac{C^2}{4\pi^2 (1 - Cv^2/\Lambda^2)^2} \frac{\phi^4}{4}. \end{aligned} \quad (20)$$

The shape of this modified potential is determined by the free parameters C and Λ . The latter is a scale that sets the energy at which the effect of the modified functional measure starts to become sensitive. On the other hand, C parameterizes the deviation from the usual case, when the measure is trivial. Indeed, it is easy to notice that the Standard Model Higgs potential is recovered for $C = 0$. The role of C for a fixed value of Λ is exemplified in figure 1.

To better understand the impact of these new contributions to the effective potential, let us denote by $V_{\text{measure}}(\phi)$ the new terms arising from the modified measure, i.e. the last three rows of eq. (20). Denoting $t \equiv C\phi^2/\Lambda^2$ and $t_0 \equiv Cv^2/\Lambda^2$ to simplify the notation, it is easy to see that

$$V_{\text{measure}} = -\frac{\Lambda^4}{8\pi^2} \left[\ln(1-t) + \frac{t^2 + 2t - 4tt_0}{2(1-t_0)^2} \right], \quad (21)$$

and that the derivative of this potential has the form

$$\frac{\partial V_{\text{measure}}}{\partial \phi} = \frac{\Lambda^2}{4\pi^2} C \phi \frac{(t-t_0)^2}{(1-t)(1-t_0)^2}. \quad (22)$$

For $C > 0$ and $0 < \phi < \Lambda/\sqrt{C}$, one has $0 < t < 1$ and $\partial V_{\text{measure}}/\partial \phi > 0$. Since $V_{\text{measure}}(0) = 0$, this means that V_{measure} will always lead to a *positive* contribution to the effective potential in this range of ϕ , thus *raising* it relative to the SM case. Moreover, this ϕ range must

⁵ Notice that eq. (1) involves the Euclidean action, so a positive contribution to $-S[\varphi]$, as in eq. (13), corresponds to a negative contribution to the effective potential.

⁶ The second derivative of the effective potential coincides with the physical mass, which is defined by the propagator's pole. By means of Eq. (2), the physical mass m_h is cutoff-independent.

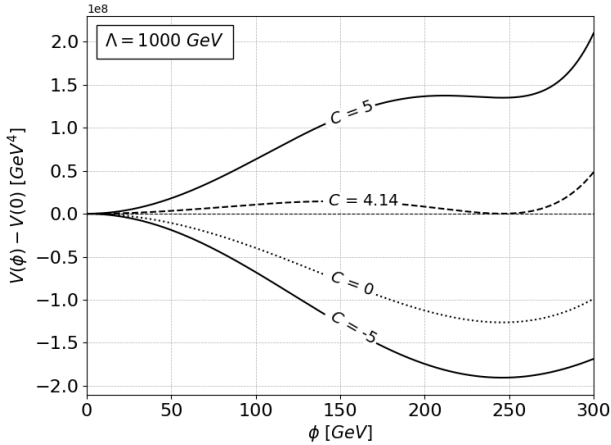


Figure 1. Normalized shapes of the potential at zero temperature for different values of C for a given $\Lambda = 1000$ GeV. The dotted line ($C = 0$) corresponds to the SM potential. For $C < 0$ the curve is always below the SM one. For $C > 0$ the curve rises above the SM in the range $\phi < \Lambda/\sqrt{C}$. Note that for $C > C_c(\Lambda = 1000 \text{ GeV}) \approx 4.14$ the symmetry-breaking vacuum is not a global minimum and spontaneous symmetry breaking would not take place.

include the minimum $\phi = v$ in order for the logarithm to be real up to this point, as we will discuss shortly. Thus, the minimum of the potential is also raised as C increases. It is well-known that this tends to lead to stronger first-order phase transitions in the early Universe [35]. For this reason we will henceforth limit ourselves to the case⁷ $C > 0$.

One can immediately impose a few constraints on these parameters from simple consistency conditions of the theory and also from LHC bounds on the scalar sector.

Existence of electroweak symmetry breaking: From figure 1 one sees that, for a fixed Λ , there is a certain critical value $C_{\text{noEWSB}}(\Lambda)$ above which the global minimum is at $\phi = 0$ rather than at $\phi = v$, even at zero temperature. This would mean that symmetry breaking would never have taken place. This should be avoided, so we impose

$$C < C_{\text{noEWSB}}(\Lambda). \quad (23)$$

Stability of the field configuration with vev ϕ : By simple inspection one can see that, for $C > 0$, the zero-temperature potential becomes complex-valued for large enough values of the field ϕ . This means that the quantum state whose vev is this ϕ will actually be an unstable state and will eventually decay [36]. In order to avoid such complications in the field range of our interest, we require the argument of the logarithm to be positive

at least for $\phi \leq \phi_{\text{stab}}$ with $\phi_{\text{stab}} \geq v$. Fixing this ϕ_{stab} then gives an upper bound

$$C < \left(\frac{\Lambda}{\phi_{\text{stab}}} \right)^2. \quad (24)$$

Vacuum stability: In principle one could also wonder about the possibility that the broken vacuum $\phi = v$ is not the deepest minimum of the potential, which would lead to the possibly catastrophic situation of an unstable vacuum. From eq. (20) one sees that, for $C > 0$, this may indeed be the case (though not necessarily), since for large field values the potential becomes effectively

$$V^{(1)}(\phi \rightarrow \infty, 0) \rightarrow \lambda_{\text{eff}} \frac{\phi^4}{4}, \quad (25)$$

with

$$\lambda_{\text{eff}} = \frac{m_h^2}{2v^2} + \sum_i \frac{n_i g_i^4}{16\pi^2} \ln \frac{\phi^2}{v^2} - \frac{C^2}{4\pi^2} \left(1 - \frac{Cv^2}{\Lambda^2} \right)^{-2}. \quad (26)$$

However, we have shown above that, in the range $0 < \phi < \Lambda/\sqrt{C}$, the new terms V_{measure} can only *raise* the SM potential. So the unboundedness of $V^{(1)}$ from below will only be relevant in the region where $V^{(1)}$ becomes complex and the state with vev ϕ is itself unstable, as discussed above. Moreover, the real part of the potential, which describes the energy density of the field configuration, displays an arbitrarily large barrier before we enter the problematic unstable region, so tunneling to the unstable state is highly suppressed. For this reason we will not pursue the consequences of this condition any further.

Bounds on the Higgs self-coupling: The model in consideration adds corrections to the Higgs trilinear coupling. The Higgs $H = \phi - v$ has a cubic self-interaction through the term $\lambda v H^3$, where, in the Standard Model, $\lambda_{\text{SM}} = m_h^2/(2v^2)$. Our model modifies this value, such that an effective trilinear coupling is achieved with $\lambda_{\text{eff}} = \kappa_\lambda \lambda_{\text{SM}}$. Using the fact that

$$\lambda_{\text{eff}} = \frac{1}{6v} \left. \frac{\partial^3 V}{\partial \phi^3} \right|_{\phi=v} \quad (27)$$

we obtain

$$\kappa_\lambda = 1 + \sum_i \left(\frac{n_i g_i^4}{24\pi^2} \frac{v^2}{m_h^2} \right) + \frac{2v^4}{3\pi^2 m_h^2 \Lambda^2} \left(\frac{C}{1 - \frac{Cv^2}{\Lambda^2}} \right)^3. \quad (28)$$

The current 68% C.L. limits on the Higgs trilinear coupling are $1.1 \leq \kappa_\lambda \leq 4.8$ [37]. These were obtained from diHiggs + single Higgs production while keeping all the other couplings fixed at the SM values, as is appropriate for the case under consideration here.

IV. THERMAL EFFECTIVE POTENTIAL AND THE ELECTROWEAK PHASE TRANSITION

We now consider the effects of finite temperature on the effective potential. The 1-loop thermal correction is

⁷ We have explicitly checked that no strongly first-order phase transitions occur for $C < 0$.

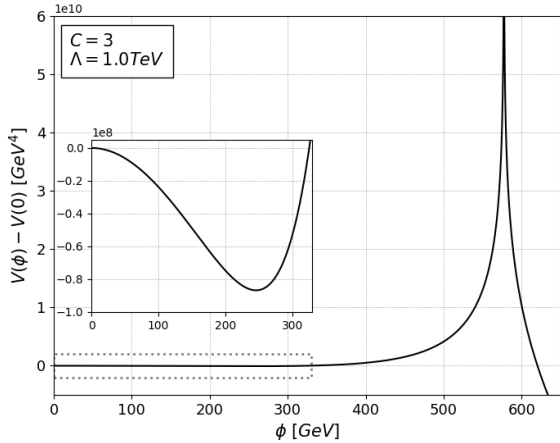


Figure 2. Normalized shape of the potential at zero temperature for $\Lambda = 1$ TeV and $C = 3$. The region in the dotted line correspond to the area in the zoom. In the figure one can see the infinity barrier at $\phi = \frac{\Lambda}{\sqrt{C}} \approx 577$ GeV that assures that a transition will never occurs after achieved the currently vacuum value.

well known in the literature [38–40] and is given by

$$\begin{aligned} \Delta V^{(1)}(\phi, T) &= \frac{T^4}{2\pi^2} \sum_{i=\text{boson}} n_i J_B \left(\frac{m_i(\phi)^2}{T^2} \right) \\ &\quad - \frac{T^4}{2\pi^2} \sum_{i=\text{fermion}} n_i J_F \left(\frac{m_i(\phi)^2}{T^2} \right) \\ &\quad - \frac{T}{12\pi} \cdot 3 (m_L^3(\phi, T) - m_L^3(\phi, 0)), \end{aligned} \quad (29)$$

where we are again summing over all fermionic and bosonic contributions, and $J_{B,F}$ are numerically evaluated functions defined by the integrals

$$J_{B,F}(y) = \int_0^\infty x^2 \ln(1 \mp e^{-\beta\sqrt{x^2+y^2}}), \quad (30)$$

with $-$ (resp. $+$) corresponding to bosonic (resp. fermionic) contributions. The third line in eq. (29) are the so-called daisy terms, which introduce thermal corrections to the mass of the longitudinal components of the gauge bosons in order to improve the loop expansion. For our model, with a SM-like particle content, we have [40] $m_L^2(\phi, T) = \frac{1}{4}\bar{g}^2\phi^2 + \frac{11}{6}\bar{g}^2T^2$ with $\bar{g}^2 = 4(m_W^2(v) + m_Z^2(v))/(3v^2)$.

The full effective potential is thus:

$$V^{(1)}(\phi, T) = V^{(1)}(\phi, T=0) + \Delta V^{(1)}(\phi, T). \quad (31)$$

In the early universe, for sufficiently high temperatures, the thermal part of the potential is proportional to $+T^2\phi^2$ and dominates over the negative quadratic terms in eq. (20). In this case all contributions to the effective potential are positive, and there is only one minimum

at $\phi = 0$: one says that electroweak symmetry is restored. As the Universe cools down, eventually a second minimum appears and becomes energetically degenerate with $\phi = 0$: this is the so-called critical temperature of the electroweak phase transition, $T_c \sim \mathcal{O}(100)$ GeV. Below this temperature the Universe goes through a phase transition in which the Higgs vev ϕ acts as the order parameter. It is known that, for the Standard Model, this process is actually a smooth crossover [41]. We will show that the MMFMM could lead to a strong first order phase transition for sufficiently large $C > 0$.

With that in mind, we proceed to compute the relevant parameters following the standard procedures [39, 42, 43]. Below the critical temperature there will be a probability that the Higgs field will transition from the symmetric state $\phi_s = 0$ to the broken state $\phi_b \neq 0$. This will happen via the nucleation of bubbles of the broken phase in a universe filled with the symmetric state. The rate at which the bubbles will be nucleated per unit volume is

$$\Gamma \approx A(t)e^{-S_3/T}, \quad (32)$$

with the 3D Euclidean action

$$S_3[\phi] = \int d^3x \left[\frac{1}{2}(\nabla\phi)^2 + (V(\phi, T) - V(0, T)) \right]. \quad (33)$$

In principle the rate in eq. (32) would include a sum over all configurations mediating the transition between the two vacua, but because of the exponential suppression the dominant contribution will come from the configuration that actually minimizes the action [44]. It can also be shown that the minimal energy configuration is spherically symmetric [45], so the Euler-Lagrange equations for the configuration that minimizes the action (33) is

$$\frac{d^2\phi}{dr^2} + \frac{2}{r} \frac{d\phi}{dr} - \frac{\partial V}{\partial\phi}(\phi, T) = 0 \quad (34)$$

with boundary conditions

$$\phi'(0) = 0, \quad \phi(0) \neq 0, \quad \phi(r \rightarrow \infty) = 0 \quad (35)$$

to ensure that the configuration indeed interpolates the two vacuum states.

We solve this equation using a custom-made Python code implementing a shooting method, with a bisection algorithm applied for finding the initial condition $\phi(0)$ which will lead to the desired behaviour of $\phi(r \rightarrow \infty) = 0$. Having found a solution, one can plug it back into Eqs. (33) and (32) to find the nucleation rate per unit volume, which then allows us to compute the number of nucleated bubbles per Hubble horizon. The nucleation temperature T_n is defined as the temperature at which this number is unity. For phase transitions occurring at the electroweak scale $\mathcal{O}(100)$ GeV this condition essentially reduces to [43]

$$\frac{S_3(T_n)}{T_n} \approx 140. \quad (36)$$

This is the criterium we use to find T_n .

There are two other parameters that can be calculated from equilibrium considerations alone (i.e. from the knowledge of the effective potential and the relevant transition temperature). One is often called the transition strength parameter, and is a measure of the energy budget of the transition:

$$\alpha = \frac{1}{\rho_r} \Delta \left(V^{(1)}(\phi, T) - \frac{1}{4} T \frac{\partial V^{(1)}}{\partial T} \right) \Big|_{T=T_n} \quad (37)$$

where Δ corresponds to the difference between the expression in parenthesis at the symmetric and the broken minima at T_n , and $\rho_r = g_* \pi^2 T_n^4 / 30$ is the energy density due to radiation from relativistic species⁸. Notice that the quantity in parenthesis is the trace anomaly $\theta = (\text{trace of energy-momentum tensor of the plasma})/4 = (e - 3p)/4$, where $e = T \partial p / \partial T - p$ is the energy of the plasma and $p = -V^{(1)}(\phi, T)$ its pressure. The definition of this parameter varies across the literature, with the trace anomaly being replaced by either e or $-p$ in some cases⁹ [47] and the denominator ρ_r being replaced by $3/4$ of the enthalpy $3w_f/4$ in other cases. A discussion of these different uses can be found in [46].

Another relevant parameter is the (inverse) characteristic time scale of the transition, which can be computed as [42, 48]

$$\frac{\beta}{H_*} = T_n \frac{dS_3}{dT} \Big|_{T=T_n}. \quad (38)$$

From this one computes the average size of the colliding bubbles as $R_* \equiv (8\pi)^{1/3} v_w \beta^{-1}$ (with v_w the bubble expansion velocity) [49], so one expects the GW spectrum to be proportional to $v_w \beta^{-1}$.

The calculation of the bubble expansion velocity depends on an adequate estimate of the counter-pressure against the expanding wall, which has an equilibrium as well as a non-equilibrium contribution. To find the latter one needs to solve the integro-differential Boltzmann equation, which is only well-defined once we know how to compute the collision terms. There are various approaches to this issue, ranging from a fully numerical solution of the Boltzmann system on a lattice [50], an expansion of the non-equilibrium fluctuations in Chebyshev polynomials [51] allied with a collocation method for solving the Boltzmann system (and a fully numerical computation of the collision terms), or a fluid Ansatz for the

fluctuations [52–54] (which allows for an analytic calculation of the collision terms at leading-log [55]) together with a procedure for taking moments to reduce the Boltzmann equation to a linear system of ODEs. Regardless of the approach chosen, the full setup also requires solving the hydrodynamical equations to determine whether the wall front expands as a deflagration, a hybrid or a detonation [56]. Overall, regardless of which approach is chosen, one can safely say that finding v_w is a highly non-trivial matter¹⁰. In this work we assume for simplicity that $v_w \approx 1$, which is typically within the correct order of magnitude of full results for models with a Standard Model particle content and transitions strengths of the order considered here [53, 54].

V. GRAVITATIONAL WAVES

After nucleating, bubbles expand and eventually collide, filling the entire Universe with the broken phase. This happens at a characteristic temperature called percolation temperature $T_* < T_n$, defined as the temperature at which about 30% of the Universe is filled by the true vacuum [58]. These collisions break the sphericity of the bubbles, inducing a time-varying quadrupole moment of energy-momentum which sources gravitational waves. It is at this point that a stochastic GW spectrum is produced. This means that the relevant temperature for computing the phase transition parameters should actually be the percolation temperature T_* . However, one typically has $T_* \approx T_n$, and this is the approximation we will use, which holds for non-supercooled transitions like the ones considered here. For this reason Eqs. (37) and (38) have been defined at T_n .

For phase transitions that nucleate and percolate at a finite temperature, there are two main sources of gravitational waves¹¹, namely sound waves and turbulence (i.e. linear and nonlinear perturbations) in the plasma [42, 43, 48]. It is known that these spectra satisfy a broken power-law and have a peak at a characteristic frequency $\sim \mathcal{O}(\text{few mHz})$, so we will parametrize it as

$$h^2 \Omega(f) = h^2 \Omega^{(\text{peak})} \times S(f), \quad (39)$$

with Ω the ratio of energy density in GWs over the critical density of our Universe. This critical density is proportional to the square of the Hubble constant today,

⁸ Since we are not altering the Standard Model field content, the number of relativistic degrees of freedom at the electroweak phase transition is $g_* = 106.75$.

⁹ Refs. [46, 47] also discuss the possibility of using another generalization of α , by letting the trace anomaly depend on the speed of sound: $\hat{\theta} = 1/4(e - p/c_s^2)$. This reduces to our definition when $c_s = 1/\sqrt{3}$, the speed of sound obtained from the bag model for the plasma, which is the case considered here.

¹⁰ See ref. [57] for a recent numerical code for computing the collision terms and finding v_w for any given model, using the collocation method and an expansion in Chebyshev polynomials.

¹¹ In principle there would also be a contribution from the kinetic energy in the scalar field itself. This is most important in the case of runaway bubbles, when the counter-pressure is never enough to stop the walls from accelerating indefinitely. Recent calculations show that this happens less often than previously expected [59–62], so we choose to neglect the scalar contribution to the spectrum.

$H_0^2 = (100h \text{ km/s/Mpc})^2$. The value of h still carries a large uncertainty due to tensions in measurements from cosmological data and from supernovae. To avoid the impact of these uncertainties on the GW spectrum, it is common to actually write the GW energy density in terms of $h^2\Omega$ rather than Ω itself.

For the sound wave contribution the spectrum has been determined from numerical simulations¹² [63] and encapsulated in the fit [42]

$$h^2\Omega_{\text{sw}}^{\text{peak}}(f) = 2.65 \times 10^{-6} \times \left(\frac{v_w}{\beta/H_*}\right) \left(\frac{\kappa_{\text{sw}}\alpha}{1+\alpha}\right)^2 \left(\frac{100}{g_*}\right)^{\frac{1}{3}} \mathcal{Y}_{\text{sup}} \quad (40)$$

for the peak amplitude. Apart from the parameters already described above, the peak amplitude also depends on the efficiency in converting the energy released by the transition into sound waves, κ_{sw} . We will use the one for non-runaway phase transitions [42, 48]:

$$\kappa_{\text{sw}} = \frac{\alpha}{0.73 + 0.83\sqrt{\alpha + \alpha}}. \quad (41)$$

Moreover, in equation (40) we have also included a suppression factor \mathcal{Y}_{sup} (as compared to the result quoted in ref. [42]) to account for the possibility that the sound waves die off into turbulence before a Hubble time. This was not included in the initial simulations of refs. [63, 64], which assume long-lasting sound waves, but it turns out that in typical models this is not a reasonable assumption and sound waves will typically decay at a characteristic time [65, 66]

$$\tau_{\text{sw}}H_* = (8\pi)^{\frac{1}{3}} \frac{v_w}{\beta/H_*} \sqrt{\frac{4}{3} \frac{1+\alpha}{\kappa_{\text{sw}}\alpha}}. \quad (42)$$

We will then model this suppression factor as

$$\mathcal{Y}_{\text{sup}} = \min\{1, \tau_{\text{sw}}H_*\}. \quad (43)$$

Equation (40) provides only an expression for the peak of the spectrum. Its shape is given by

$$S_{\text{sw}}(f) = \left(\frac{f}{f_{\text{sw}}}\right)^3 \left(\frac{7}{4 + 3(f/f_{\text{sw}})^2}\right)^{7/2}, \quad (44)$$

with f_{sw} the redshifted frequency of the peak frequency as measured today,

$$f_{\text{sw}} = 1.9e - 2 \text{ mHz} \times \frac{1}{v_w} \left(\frac{\beta}{H_*}\right) \left(\frac{T_*}{100 \text{ GeV}}\right) \left(\frac{g_*}{100}\right)^{\frac{1}{6}}. \quad (45)$$

¹² These simulations have only taken into account sufficiently weak phase transitions, with $\alpha \ll 1$. Whether and how the spectra would change for stronger transitions remains an open issue. However, as will be seen in figure 6 below, in this model we are most often in the region of $\alpha \lesssim 1$.

The GW spectrum produced from turbulence in the plasma is often computed in the literature using the fit found in ref. [42],

$$h^2\Omega_{\text{turb}}^{\text{peak}}(f) = 3.35 \times 10^{-4} \times \left(\frac{v_w}{\beta/H_*}\right) \left(\frac{\kappa_{\text{turb}}\alpha}{1+\alpha}\right)^{\frac{3}{2}} \left(\frac{100}{g_*}\right)^{\frac{1}{3}}, \quad (46)$$

with shape

$$S_{\text{turb}} = \frac{(f/f_{\text{turb}})^3}{[1 + (f/f_{\text{turb}})]^{\frac{11}{3}} \left(1 + 8\pi \frac{f}{h_*}\right)}. \quad (47)$$

The h_* term in the equation corresponds to the Hubble parameter at the epoch of the phase transition, rescaled by the cosmological redshift to relate it to the present time, and is defined as

$$h_* = 16.5 \times 10^{-3} \text{ mHz} \left(\frac{T_*}{100 \text{ GeV}}\right) \left(\frac{g_*}{100}\right)^{\frac{1}{6}}, \quad (48)$$

and f_{turb} is the peak frequency measured today,

$$f_{\text{turb}} = 2.7e - 2 \text{ mHz} \times \frac{1}{v_w} \left(\frac{\beta}{H_*}\right) \left(\frac{T_*}{100 \text{ GeV}}\right) \left(\frac{g_*}{100}\right)^{\frac{1}{6}}. \quad (49)$$

We emphasize, however, that the GW spectrum from turbulence is actually still a matter of intense investigation [43]. Even if one is willing to use the expression above, one would need to know the efficiency factor κ_{turb} , corresponding to the fraction of released energy that is actually converted to turbulence. There is so far no appropriate modeling for this parameter. It is sometimes assumed that $\kappa_{\text{turb}} = \varepsilon\kappa_{\text{sw}}$, with typical values ranging from 5 – 10% [42, 48, 67]. Sometimes extreme cases as $\varepsilon = 0$ (negligible turbulence) [43] and $\varepsilon = 1$ [68] are also assumed. In the next section we will show how the spectrum changes if we vary ε from 0 to 1.

Analysis of detectability

To assess the detectability of these GWs one must calculate the *signal-to-noise ratio* (SNR), obtained by comparing the predicted signal, $\Omega_{\text{theory}}(f)$, to the noise spectrum of a given interferometer, $\Omega_{\text{noise}}(f)$, and integrating this ratio over the operational time of the experiment. Moreover, due to the broadband nature of the stochastic GW spectrum from phase transitions, it is also important to integrate this ratio over all frequencies accessible at the experiment, since an accumulation of small $\Omega_{\text{theory}}(f)/\Omega_{\text{noise}}(f)$ could still yield a large enough SNR when summed over. If the spectrum has a power-law shape, $\Omega_{\text{theory}}(f) = \Omega^{\text{peak}} f^n$, ref. [69] provided a recipe for constructing the so-called *power-law integrated sensitivity curves* (PLISCs) by varying the power n and calculating the value of Ω^{peak} for which the spectrum would

be detectable ($\text{SNR} > 1$). This would yield an envelope of straight lines in a log-log plot of Ω vs f , such that the actual spectrum (if it has a power-law shape) would be detectable if its curve lies *above* this envelope. This provides a convenient graphical way of displaying detectability results.

But from eqs. (44) and (47) one sees that the spectrum from cosmological phase transitions is not a simple power-law, but a broken power law with a peak. In this case the comparison of the spectrum with the PLISCs would only be plausible if the peak lies beyond the range of detectability of the experiment, such that the spectrum would effectively have a simple power-law shape as far as this experiment is concerned. This is a too restrictive requirement, and it would be useful to have another reliable, simple and graphical way to assess the detectability of a generic broken power-law spectrum as predicted by phase transitions.

Now, because the shape of these spectra is known, given e.g. by eqs. (44) and (47), the integral of $\Omega_{\text{theory}}(f)/\Omega_{\text{noise}}(f)$ can be readily performed, and one can rewrite the condition $\text{SNR} > 1$ in terms of a condition on the minimal Ω^{peak} that would yield the spectrum detectable (as a function of the peak frequency). This new method was recently developed in ref. [48] and is dubbed the *peak integrated sensitivity curves* (PISCs). This provides a reliable graphical way of displaying detectability results for cosmological GW backgrounds. The disadvantage, compared to the PISCs, is that this method is only applicable for a comparison of the peak amplitude, and all information on the spectral shape has been integrated over.

In what follows we will use mostly the PISC method for checking an $\text{SNR} > 1$, except in one case when the full spectral shape is shown for illustrative purposes. We will then also use this opportunity to briefly emphasize the advantage of the PISC over the PLISC method for studying cosmological phase transitions.

VI. RESULTS

Our task is to evaluate the possibility of using gravitational wave detectors to probe deviations in the scalar potential arising from terms of the form $\sim \Lambda^4 \log(1 - C\phi^2/\Lambda^2)$ (cf. eq. (21)). For this purpose, we have performed a scan over the (Λ, C) parameters, with $\Lambda \in (500, 3000)$ GeV, evaluating the phase transition parameters and the GW spectrum.

Figure 3 illustrates the behaviour of the ratio ϕ_n/T_n , i.e. the order parameter (Higgs VEV) per temperature at the start of bubble nucleation, which serves as a measure of how strongly first order the phase transition is. As expected, for fixed Λ the transition becomes stronger as we increase C . This is because for $C > 0$ the minimum of the potential is raised compared to the SM case, as discussed previously in section III, so we need smaller temperature corrections to reach the critical (and also the

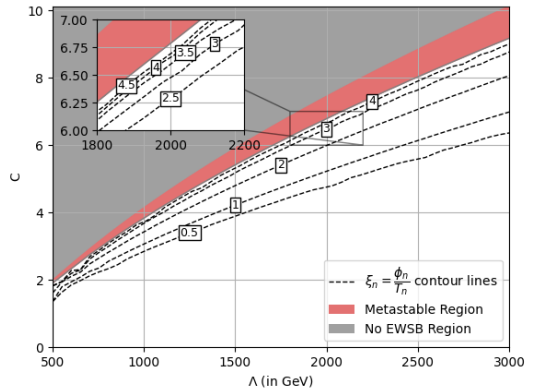


Figure 3. Contour plot for the values of the transition strength parameter $\xi_* = \phi_*/T_*$ in the (Λ, C) plane. The figure illustrates clearly how increasing C leads to stronger phase transitions, as expected from the raising of the zero-temperature minimum shown in figure 1.

nucleation) temperature. Since the VEV also decreases with T , a smaller transition temperature means larger ϕ/T [35].

If C is large enough one finds that the condition $S_3/T \approx 140$ in eq. (36) is never satisfied. This means we never guarantee the nucleation of one bubble per Hubble horizon. We interpret this as a condition that the transition will not complete, i.e. the false vacuum is *metastable*¹³. As we increase C even further we eventually raise the electroweak minimum above the symmetric phase even at $T = 0$: this means that symmetry breaking would never have taken place. The *metastability* region is shown in red in Fig. 3 (and in light gray in the following figures), and the region of *no electroweak symmetry breaking* is shown in dark gray here and in the following plots.

Once a certain point (Λ, C) passes all the physicality constraints discussed in section III, we can calculate the transition parameters and the GW spectrum. Figure 4 illustrates typical shapes of this spectrum for a fixed $\Lambda = 1000$ GeV and differing values of C . As expected, the amplitude increases with C , because the transition gets stronger. Solid lines correspond to the contribution of sound waves only, whereas dashed lines include the contribution from turbulence with an extreme efficiency factor of $\kappa_{\text{turb}} = \kappa_{\text{sw}}$ (or $\varepsilon = 1$). The result shows that

¹³ Note that, in a radiation-dominated Universe, bubbles might expand faster than the Hubble rate, so a bubble might grow beyond the Hubble volume at which it was nucleated, and the transition could complete even with less than one bubble per horizon [58]. The condition of metastability is actually less stringent, namely that there must be less than $\sim \mathcal{O}(0.1)$ bubbles per horizon [58], which in practice changes very little the exclusion regions we obtain here. Thus we choose to keep the usual condition of at least one nucleated bubble per horizon.

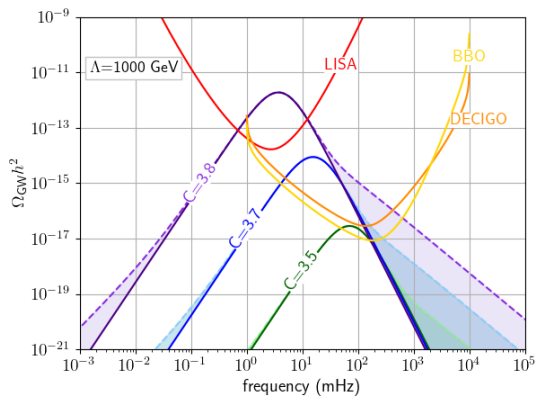


Figure 4. Typical gravitational wave spectra for a fixed value of $\Lambda = 1000$ GeV and various C . The spectra exhibit contributions from two different sources: the solid lines represent contributions from sound waves, while the dashed lines illustrate the contribution from turbulence assuming an efficiency factor $\varepsilon = 1$ (see text). The shaded region is the range obtained by varying ε from 0 to 1. Sensitivity curves of the different GW detectors are power-law-integrated sensitivity curves (PLISCs) [69] taken from [48]. See the main body of the text for a discussion on these sensitivity curves.

turbulence changes the spectrum mostly in its tails, but does not significantly affect the peak. For this reason, and because any choice of ε would be rather arbitrary, in the following discussions we will instead completely neglect the turbulence contribution, setting $\varepsilon = 0$. Note that this will lead to a *more conservative* estimate of how sensitive GW detectors are to this model.

We also show in figure 4 the power-law integrated sensitivity curves (PLISC) [69] of three different detectors, namely LISA, DECIGO and BBO. As illustrated, it is not typically true that the spectrum has a simple power law shape for the whole detectability range of these experiments. Thus, looking at figure 4 alone is in principle not enough to judge whether the spectrum is detectable¹⁴. We will henceforth use the PISC method to assess the detectability of these GWs.

Peak amplitudes from the sound wave contributions to the GW spectrum are shown in fig. 5 together with the corresponding PISCs for LISA, DECIGO and BBO. The figure illustrates the behaviour of the spectrum as we vary the parameters Λ and C . For a fixed Λ , varying the parameter C by a few % can change the position of the peak amplitude by 2 orders of magnitude. Conversely, if we double the value of Λ , the value of C has to be approximately doubled as well in order to keep the peak

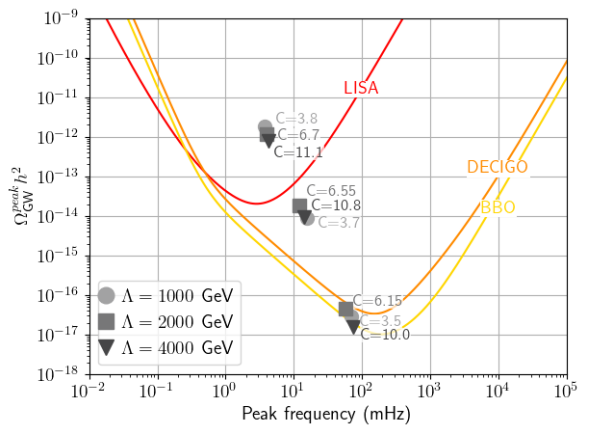


Figure 5. Peak amplitudes of the gravitational wave spectra due to sound waves only, for different values of Λ and C . The sensitivity curves of the detectors are peak-integrated sensitivity curves (PISC) [48].

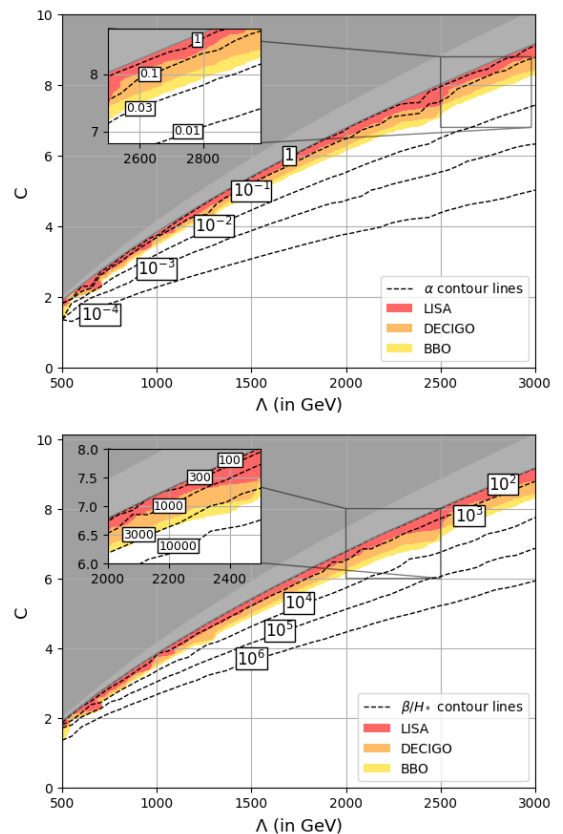


Figure 6. Contour plot for (above) α and (below) β in the (Λ, C) plane. Colored regions correspond to points within detectability range of different interferometers (obtained by requiring the theoretical amplitude to be larger than the PISC at the peak frequency). The gray regions for larger values of C correspond to the region of metastability (light) and lack of symmetry breaking at $T = 0$ (dark gray).

¹⁴ We reinforce that these PLISCs were constructed by assuming that the spectrum would keep increasing for all f . The fact that the power law is broken, and that the spectrum at some point decreases, means that the integral of $\Omega_{\text{theory}}(f)/\Omega_{\text{noise}}(f)$ would actually be smaller than for a power-law, and the comparison with the PLISC is not totally appropriate.

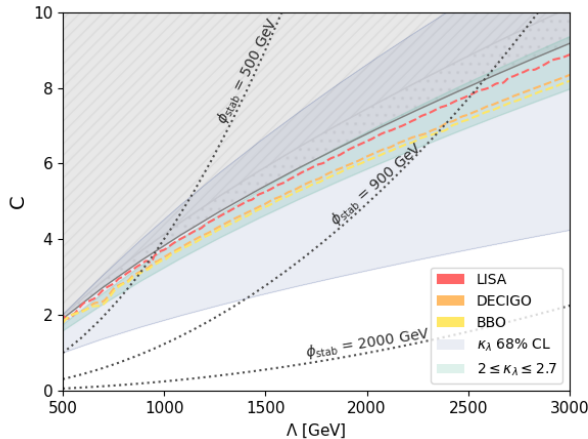


Figure 7. Dashed curves show the values of C and Λ for which this model predicts a cosmological gravitational wave background with $\text{SNR} = 1$ at LISA, DECIGO and BBO. The gray dotted lines represent the values of ϕ_{stab} at which the potential becomes complex-valued. Also shown are the currently allowed region from 68% C.L. bounds on the Higgs trilinear coupling. This region is much wider than the parameter range assessible at GW interferometers, which corresponds to $2 \leq \kappa_\lambda \leq 2.7$. The hashed regions at larger values of C indicate metastability (dotted) and lack of symmetry breaking at $T = 0$ (hashed bars).

amplitude at the same position. Thus the spectrum is much more sensitive to C than to Λ . This can be understood from the following perspective. In this model we are merely altering the shape of the effective potential, leaving all the other sectors as in the SM, so we expect all the new physics to be encapsulated in the scalar field's self-couplings. Looking e.g. at eq. (28) one sees that the trilinear¹⁵ is much more sensitive to a change in C than to Λ , as it behaves like $\kappa_\lambda = 1 + \kappa_{1\text{-loop}}^{\text{SM}} + \frac{\text{cnst.}}{\Lambda^2} \left(\frac{C}{1 - C v^2 / \Lambda^2} \right)^3$. The new physics contributions to this coupling roughly scales with Λ as Λ^{-2} , whereas an enhancement in C not only boosts this contribution by a factor C^3 in the numerator, but it also decreases the (cubed!) denominator, leading to a further enhancement factor.

It is also interesting to investigate the typical values of α and β that lead to a detectable GW spectrum, as well as the associated values of C and Λ . This is shown in figure 6. One notes that BBO could start probing the phase transition for mild values of $\alpha \gtrsim 0.03$ and $\beta/H_* \gtrsim 3000$. However, detectability at LISA requires rather extreme values of $\alpha \sim 1$ and $\beta/H_* \sim \text{few} \times 100$. Such values are within reach of the model under study, but then the parameters would be rather close to the forbidden region

¹⁵ Recall that the trilinear is the first coupling to be modified by the new physics, since we have renormalized the potential such that its first and second derivatives remain unaltered at the minimum.

of metastability. This means that, if LISA would be able to probe GWs from this model, it would also be able to establish a stringent constrain on C vs. Λ .

Our main results are summarized in figure 7, illustrating how GW detectors and current/near-future colliders would fare in probing such a logarithmic modification in the scalar effective potential. Again we show the excluded regions (gray hashed) due to metastability of the false vacuum and no symmetry breaking. Also shown are the $\text{SNR} = 1$ curves for LISA, DECIGO and BBO. The dotted lines correspond to the regions where the state $\langle \phi \rangle$ becomes unstable at a certain energy level ϕ_{stab} , as discussed in section III. Requiring stability up to 2 TeV excludes most of the interesting region, but a stable state up to 500 – 1000 TeV would still allow for a substantial slice of the parameter space. Nevertheless, one sees that this condition clearly establishes an important constraint on the model. Even if this state is not stable, a more detailed analysis would be required to establish its actual decay time, which could still be longer than the age of the Universe and therefore safe. This is however beyond the scope of the current work, and we will deem satisfactory the fact that some regions are still allowed in the ~ 1 TeV energy range.

Most interesting in this figure is the wide blue region showing the 68% C.L. bounds on the Higgs trilinear coupling, $1.1 \leq \kappa_\lambda \leq 4.8$ [37]. Notice how the GW sensitivity curves are well within this region: this means that, should a spectrum be detected and traced to a modification in the scalar potential alone, then these experiments would yield much more precise bounds on the trilinear than current colliders. For comparison we also show that the sensitivity of these GW detectors roughly corresponds to the region of $2.0 \leq \kappa_\lambda \leq 2.7$, i.e. an uncertainty $\delta\kappa_\lambda \equiv \kappa_\lambda - 1 \lesssim 1.7$. This level of uncertainty is expected to be reached only by future lepton colliders operating at 350 GeV and 200 fb^{-1} luminosity, or a combination of the HL-LHC plus a lepton collider [10]. We recall, however, that LISA is already a funded project with launch date for the mid 2030s, whereas unfortunately no lepton colliders have reached such an advanced stage yet. Thus, GW detectors could play an important role in tightening current constraints on Higgs self-couplings.

VII. CONCLUSIONS

In this work we have investigated the capabilities of collider experiments and GW detectors in probing deviations of the SM affecting the scalar potential only. For this purpose we have considered the so-called MMFMM (of *minimal modified functional measure model*), a model where this modification stems from a Riemannian definition for the functional integration measure, which would lead to a new logarithmic correction to the Higgs effective potential. However, we expect our results to be qualitatively correct for any model where the BSM physics affects the scalar self-couplings alone.

Our main conclusions are as follows. First, we have seen that there is a strong correlation between the scalar self-couplings (in particular the trilinear) and the condition of detectability of a stochastic GW background produced by a cosmological phase transition. In other words, should the trilinear be sufficiently large (here $\kappa_\lambda \gtrsim 2$), then the GW spectrum shall be detectable at future interferometers such as LISA, DECIGO and BBO ($\text{SNR} > 1$). This is not unexpected: if the only new physics is in the scalar sector, then all its effects (including the phase transition strength and the resulting GW spectrum) should be encapsulated in the self-couplings.

Secondly, this means we could use these experiments as a probe of the scalar self-coupling, and it is worth noticing that GW detectors will be probably launched sooner than collider counterparts with similar capabilities. We are entering an era in which GW experiments are receiving increasing attention (and funding), because we have just started probing this spectrum and, being still largely unexplored, it still contains enormous potential of new (potentially groundbreaking) discoveries. It is thus essential that we exploit these experiments with the purpose of probing particle physics as well, rather than relying only on colliders and direct detection. In a recent work we have shown that GW experiments and colliders/detectors could offer complementary results when the new physics lives in a dark sector [7]. Here we show instead how *competitive* they can be with each other in probing the scalar sector, assuming everything else remains SM-like.

Our quantitative results are obviously strongly dependent on the particular model we studied. However, we expect them to be qualitatively valid regardless of model details, *as long as only the scalar sector is modified*. Too large self-couplings would lead to stronger transitions

and larger GW spectra, until an upper limit is reached where the model becomes unphysical (e.g. failing to lead to a successful symmetry breaking mechanism). The LISA detectability bound is often very close to this upper bound, meaning that either LISA does not see the transition, or, if it does, it also constraints the self-coupling to a very decent accuracy. Other detectors could be sensitive to even lower values of the trilinear, closer to the SM value, therefore leading to its measurement with even better precision.

As a final remark, let us emphasize our earlier statement that *by no means GW detectors will completely obliterate the importance of colliders and direct detection experiments in the near-future*, and that it is crucial to keep investing on all these fronts, especially at this moment when we still know very little about the actual properties of the BSM physics. A detection of a stochastic GW background would allow for a (more or less) direct mapping to the thermodynamical parameters such as T, α and β [70, 71], but converting these to actual effective couplings depends on certain model assumptions. The same holds for the data collected by colliders, of course, but since they measure different observables (cross sections \times branching ratios) there is more potential for disambiguation if both sets of experiments are used at the same time.

ACKNOWLEDGEMENTS

GFV would like to thank FAPEMIG and Universidade Federal de Minas Gerais (UFMG) for financial support during the preparation of this work. IK is funded by the National Council for Scientific and Technological Development (CNPq), grant numbers 303283/2022-0 and 401567/2023-0.

-
- [1] LIGO SCIENTIFIC, VIRGO collaboration, *Observation of Gravitational Waves from a Binary Black Hole Merger*, *Phys. Rev. Lett.* **116** (2016) 061102 [1602.03837].
 - [2] LIGO SCIENTIFIC, VIRGO collaboration, *GWTC-1: A Gravitational-Wave Transient Catalog of Compact Binary Mergers Observed by LIGO and Virgo during the First and Second Observing Runs*, *Phys. Rev. X* **9** (2019) 031040 [1811.12907].
 - [3] LIGO SCIENTIFIC, VIRGO collaboration, *GWTC-2.1: Deep extended catalog of compact binary coalescences observed by LIGO and Virgo during the first half of the third observing run*, *Phys. Rev. D* **109** (2024) 022001 [2108.01045].
 - [4] KAGRA, VIRGO, LIGO SCIENTIFIC collaboration, *GWTC-3: Compact Binary Coalescences Observed by LIGO and Virgo during the Second Part of the Third Observing Run*, *Phys. Rev. X* **13** (2023) 041039 [2111.03606].
 - [5] NANOGrav collaboration, *The NANOGrav 15 yr Data Set: Evidence for a Gravitational-wave Background*, *Astrophys. J. Lett.* **951** (2023) L8 [2306.16213].
 - [6] EPTA, INPTA: collaboration, *The second data release from the European Pulsar Timing Array - III. Search for gravitational wave signals*, *Astron. Astrophys.* **678** (2023) A50 [2306.16214].
 - [7] G. Arcadi, G. C. Dorsch, J. P. Neto, F. S. Queiroz and Y. M. Oviedo-Torres, *Probing a dark sector with collider physics, direct detection, and gravitational waves*, *Phys. Lett. B* **848** (2024) 138382 [2307.06376].
 - [8] CMS collaboration, *A portrait of the Higgs boson by the CMS experiment ten years after the discovery.*, *Nature* **607** (2022) 60 [2207.00043].
 - [9] S. Di Vita, C. Grojean, G. Panico, M. Riembau and T. Vantalon, *A global view on the Higgs self-coupling*, *JHEP* **09** (2017) 069 [1704.01953].
 - [10] S. Di Vita, G. Durieux, C. Grojean, J. Gu, Z. Liu, G. Panico et al., *A global view on the Higgs self-coupling at lepton colliders*, *JHEP* **02** (2018) 178 [1711.03978].
 - [11] M. L. Mangano, G. Ortona and M. Selvaggi, *Measuring the Higgs self-coupling via Higgs-pair production at a*

- 100 TeV p - p collider, *Eur. Phys. J. C* **80** (2020) 1030 [2004.03505].
- [12] I. Kuntz and R. da Rocha, *Transport coefficients in AdS/CFT and quantum gravity corrections due to a functional measure*, *Nucl. Phys. B* **993** (2023) 116258 [2211.11913].
- [13] I. Kuntz and A. Malagi, *Constraining the UV with the electroweak effective action*, *JHEP* **12** (2025) 210 [2404.06987].
- [14] K. G. Wilson, *The renormalization group and critical phenomena*, *Rev. Mod. Phys.* **55** (1983) 583.
- [15] K. Costello, *Renormalization and Effective Field Theory*, vol. 170. American Mathematical Society, 2022.
- [16] R. K. Unz, *Path Integration and the Functional Measure*, *Nuovo Cim. A* **92** (1986) 397.
- [17] D. J. Toms, *The Functional Measure for Quantum Field Theory in Curved Space-time*, *Phys. Rev. D* **35** (1987) 3796.
- [18] V. Moretti, *Direct zeta function approach and renormalization of one loop stress tensors in curved space-times*, *Phys. Rev. D* **56** (1997) 7797 [hep-th/9705060].
- [19] M. Hatsuda, P. van Nieuwenhuizen, W. Troost and A. Van Proeyen, *The Regularized Phase Space Path Integral Measure for a Scalar Field Coupled to Gravity*, *Nucl. Phys. B* **335** (1990) 166.
- [20] P. van Nieuwenhuizen, *Consistent anomalies from Hamiltonian path-integrals*, *Nucl. Phys. B Proc. Suppl.* **16** (1990) 605.
- [21] C. Armendariz-Picon, J. T. Neelakanta and R. Penco, *General Covariance Constraints on Cosmological Correlators*, *JCAP* **01** (2015) 035 [1411.0036].
- [22] M. Becker and M. Reuter, *Background Independent Field Quantization with Sequences of Gravity-Coupled Approximants*, *Phys. Rev. D* **102** (2020) 125001 [2008.09430].
- [23] I. L. Buchbinder and S. L. Lyakhovich, *Canonical Quantization and Local Measure of R^{**2} Gravity*, *Class. Quant. Grav.* **4** (1987) 1487.
- [24] S. Hamamoto and M. Nakamura, *Path integral measures in higher derivative gravities*, *Prog. Theor. Phys.* **104** (2000) 691 [hep-th/0005131].
- [25] B. S. DeWitt, *The global approach to quantum field theory. Vol. 1, 2nd ed.*, vol. 114. 2003.
- [26] K. Finn, S. Karamitsos and A. Pilaftsis, *Frame Covariance in Quantum Gravity*, *Phys. Rev. D* **102** (2020) 045014 [1910.06661].
- [27] G. A. Vilkovisky, *The Unique Effective Action in Quantum Field Theory*, *Nucl. Phys. B* **234** (1984) 125.
- [28] E. S. Fradkin and G. A. Vilkovisky, *On Renormalization of Quantum Field Theory in Curved Space-Time*, *Lett. Nuovo Cim.* **19** (1977) 47.
- [29] E. S. Fradkin and G. A. Vilkovisky, *S matrix for gravitational field. ii. local measure, general relations, elements of renormalization theory*, *Phys. Rev. D* **8** (1973) 4241.
- [30] K. Fujikawa, *Path Integral Measure for Gauge Invariant Fermion Theories*, *Phys. Rev. Lett.* **42** (1979) 1195.
- [31] K. Fujikawa, *Path Integral for Gauge Theories with Fermions*, *Phys. Rev. D* **21** (1980) 2848.
- [32] K. Fujikawa, *Comment on Chiral and Conformal Anomalies*, *Phys. Rev. Lett.* **44** (1980) 1733.
- [33] J. a. M. L. de Freitas and I. Kuntz, *Massive graviton from diffeomorphism invariance*, 2307.13803.
- [34] R. Casadio, I. Kuntz and R. da Rocha, *When gravitational decoupling and quantum gravity (re)unite*, 2403.13099.
- [35] G. C. Dorsch, S. J. Huber, K. Mimasu and J. M. No, *The Higgs Vacuum Uplifted: Revisiting the Electroweak Phase Transition with a Second Higgs Doublet*, *JHEP* **12** (2017) 086 [1705.09186].
- [36] E. J. Weinberg and A.-q. Wu, *Understanding complex perturbative effective potentials*, *Phys. Rev. D* **36** (1987) 2474.
- [37] ATLAS collaboration, *Constraints on the Higgs boson self-coupling from single- and double-Higgs production with the ATLAS detector using pp collisions at $s=13$ TeV*, *Phys. Lett. B* **843** (2023) 137745 [2211.01216].
- [38] M. Laine and A. Vuorinen, *Basics of Thermal Field Theory*, vol. 925. Springer, 2016, 10.1007/978-3-319-31933-9, [1701.01554].
- [39] M. B. Hindmarsh, M. Lüben, J. Lumma and M. Pauly, *Phase transitions in the early universe*, *SciPost Phys. Lect. Notes* **24** (2021) 1 [2008.09136].
- [40] J. R. Espinosa, M. Quiros and F. Zwirner, *On the nature of the electroweak phase transition*, *Phys. Lett. B* **314** (1993) 206 [hep-ph/9212248].
- [41] M. D'Onofrio and K. Rummukainen, *Standard model cross-over on the lattice*, *Phys. Rev. D* **93** (2016) 025003 [1508.07161].
- [42] C. Caprini et al., *Science with the space-based interferometer eLISA. II: Gravitational waves from cosmological phase transitions*, *JCAP* **04** (2016) 001 [1512.06239].
- [43] C. Caprini et al., *Detecting gravitational waves from cosmological phase transitions with LISA: an update*, *JCAP* **03** (2020) 024 [1910.13125].
- [44] V. Mukhanov, *Physical Foundations of Cosmology*. Cambridge University Press, Oxford, 2005, 10.1017/CBO9780511790553.
- [45] S. Coleman, *Fate of the false vacuum: Semiclassical theory*, *Phys. Rev. D* **15** (1977) 2929.
- [46] P. Athron, C. Balázs, A. Fowlie, L. Morris and L. Wu, *Cosmological phase transitions: From perturbative particle physics to gravitational waves*, *Progress in Particle and Nuclear Physics* **135** (2024) 104094.
- [47] F. Giese, T. Konstandin and J. van de Vis, *Model-independent energy budget of cosmological first-order phase transitions—A sound argument to go beyond the bag model*, *JCAP* **07** (2020) 057 [2004.06995].
- [48] K. Schmitz, *New Sensitivity Curves for Gravitational-Wave Signals from Cosmological Phase Transitions*, *JHEP* **01** (2021) 097 [2002.04615].
- [49] K. Enqvist, J. Ignatius, K. Kajantie and K. Rummukainen, *Nucleation and bubble growth in a first order cosmological electroweak phase transition*, *Phys. Rev. D* **45** (1992) 3415.
- [50] S. De Curtis, L. D. Rose, A. Guiggiani, A. G. Muyor and G. Panico, *Bubble wall dynamics at the electroweak phase transition*, *JHEP* **03** (2022) 163 [2201.08220].
- [51] B. Laurent and J. M. Cline, *First principles determination of bubble wall velocity*, *Phys. Rev. D* **106** (2022) 023501 [2204.13120].
- [52] G. D. Moore and T. Prokopec, *How fast can the wall move? A Study of the electroweak phase transition dynamics*, *Phys. Rev. D* **52** (1995) 7182 [hep-ph/9506475].
- [53] G. C. Dorsch and D. A. Pinto, *Bubble wall velocities with an extended fluid Ansatz*, *JCAP* **04** (2024) 027 [2312.02354].
- [54] G. C. Dorsch, T. Konstandin, E. Perboni and D. A. Pinto, *Non-singular solutions to the Boltzmann equation with a fluid Ansatz*, 2412.09266.

- [55] G. C. Dorsch, S. J. Huber and T. Konstandin, *On the wall velocity dependence of electroweak baryogenesis*, *JCAP* **08** (2021) 020 [2106.06547].
- [56] J. R. Espinosa, T. Konstandin, J. M. No and G. Servant, *Energy Budget of Cosmological First-order Phase Transitions*, *JCAP* **06** (2010) 028 [1004.4187].
- [57] A. Ekstedt, O. Gould, J. Hirvonen, B. Laurent, L. Niemi, P. Schicho et al., *How fast does the WallGo? A package for computing wall velocities in first-order phase transitions*, 2411.04970.
- [58] P. Athron, C. Balázs and L. Morris, *Supercool subtleties of cosmological phase transitions*, *JCAP* **03** (2023) 006 [2212.07559].
- [59] S. H"ocher, J. Kozaczuk, A. J. Long, J. Turner and Y. Wang, *Towards an all-orders calculation of the electroweak bubble wall velocity*, *JCAP* **03** (2021) 009 [2007.10343].
- [60] A. Azatov and M. Vanvlasselaer, *Bubble wall velocity: heavy physics effects*, *JCAP* **01** (2021) 058 [2010.02590].
- [61] W.-Y. Ai, X. Nagels and M. Vanvlasselaer, *Criterion for ultra-fast bubble walls: the impact of hydrodynamic obstruction*, *JCAP* **03** (2024) 037 [2401.05911].
- [62] A. J. Long and J. Turner, *Thermal pressure on ultrarelativistic bubbles from a semiclassical formalism*, *JCAP* **11** (2024) 024 [2407.18196].
- [63] M. Hindmarsh, S. J. Huber, K. Rummukainen and D. J. Weir, *Shape of the acoustic gravitational wave power spectrum from a first order phase transition*, *Phys. Rev. D* **96** (2017) 103520 [1704.05871].
- [64] M. Hindmarsh, S. J. Huber, K. Rummukainen and D. J. Weir, *Gravitational waves from the sound of a first order phase transition*, *Phys. Rev. Lett.* **112** (2014) 041301 [1304.2433].
- [65] J. Ellis, M. Lewicki and J. M. No, *On the Maximal Strength of a First-Order Electroweak Phase Transition and its Gravitational Wave Signal*, *JCAP* **04** (2019) 003 [1809.08242].
- [66] J. Ellis, M. Lewicki and J. M. No, *Gravitational waves from first-order cosmological phase transitions: lifetime of the sound wave source*, *JCAP* **07** (2020) 050 [2003.07360].
- [67] A. Alves, D. Gonalves, T. Ghosh, H.-K. Guo and K. Sinha, *Di-Higgs Production in the 4b Channel and Gravitational Wave Complementarity*, *JHEP* **03** (2020) 053 [1909.05268].
- [68] J. Ellis, M. Lewicki, J. M. No and V. Vaskonen, *Gravitational wave energy budget in strongly supercooled phase transitions*, *JCAP* **06** (2019) 024 [1903.09642].
- [69] E. Thrane and J. D. Romano, *Sensitivity curves for searches for gravitational-wave backgrounds*, *Phys. Rev. D* **88** (2013) 124032 [1310.5300].
- [70] C. Gowling, M. Hindmarsh, D. C. Hooper and J. Torrado, *Reconstructing physical parameters from template gravitational wave spectra at LISA: first order phase transitions*, *JCAP* **04** (2023) 061 [2209.13551].
- [71] LISA COSMOLOGY WORKING GROUP collaboration, *Gravitational waves from first-order phase transitions in LISA: reconstruction pipeline and physics interpretation*, *JCAP* **10** (2024) 020 [2403.03723].